Progress in Wind Engineering

Proceedings of the 8th International Conference on Wind Engineering

Part 2

ICWE

Edited by

A.G. Davenport et al.

Elsevier

Journal of Wind Engineering and Industrial Aerodynamics, 41-44 (1992) 1435–1446
Elsevier

WIND RESPONSE OF A LARGE TENSILE STRUCTURE: THE NEW ROOF OF THE OLIMPIC STADIUM IN ROME

C. Borri[a], M. Majowiecki[b], P. Spinelli[a]

[a]Dip.to di Ingegneria Civile, Università di Firenze, via S. Marta 3, I – 50139 Firenze (ITALY)

[b]Ist. di Tecnica delle Costruzioni, Università di Bologna, via Risorgimento 2, I – 40100 Bologna (ITALY)

Abstract

After the construction of the new roofing of the Olympic Stadium in Rome, a completely new numerical model has been developed with the principal aim of investigating the aerodynamic behaviour. Starting from the available data on the pressure field measured on a model tested in wind tunnel, a multi-correlated field of the wind loading has been artificially generated to study the nonlinear response in Time Domain.

1. INTRODUCTION

In this paper some experiences and remarks concerning the structural behaviour under wind of the cable roof of the Olympic Stadium in Rome are presented.

The very limited time available for wind tunnel testing and structural design has affected in some way the completeness of the tests, carried out at the Boundary Layer Wind Tunnel Laboratory of the University of Western Ontario. In fact, while the data of a quarter of the roof are completely available together with the auto and cross-spectra of measured pressures, no data on the correlation between turbulence on two different quarters are unfortunately available until now. This caused the correlation of the fluctuating pressure for the whole turbulence field to be estimated by means of an extrapolation procedure of the existing data.

The structure behaves nonlinearly and, on the other hand, wind is the most important loading condition so that the Time Domain (T.D.) approach for the analysis of the dynamic response has to be followed.

2. THE STRUCTURAL CONCEPT

The roof was inaugurated in the occasion of the last world football championship and has a quite unusual and innovative structural concept: an elliptical form with 307.98 m x 237.26 m axes, covering a 68,000 m^2 surface (Fig. 1), simply supported at the external boundary in sixteen discrete points, more or less regularly spaced, setting up a constraint unable to transmit any moment to the structure, preventing only vertical displacements.

For a functional examination of the structure three main points can be picked out: a) an external compression ring, with triangular cross section, constituted by a truss structure of tubular members; b) seventy-eight cable trusses, which arise as cantilevers

0167-6105/92/$05.00

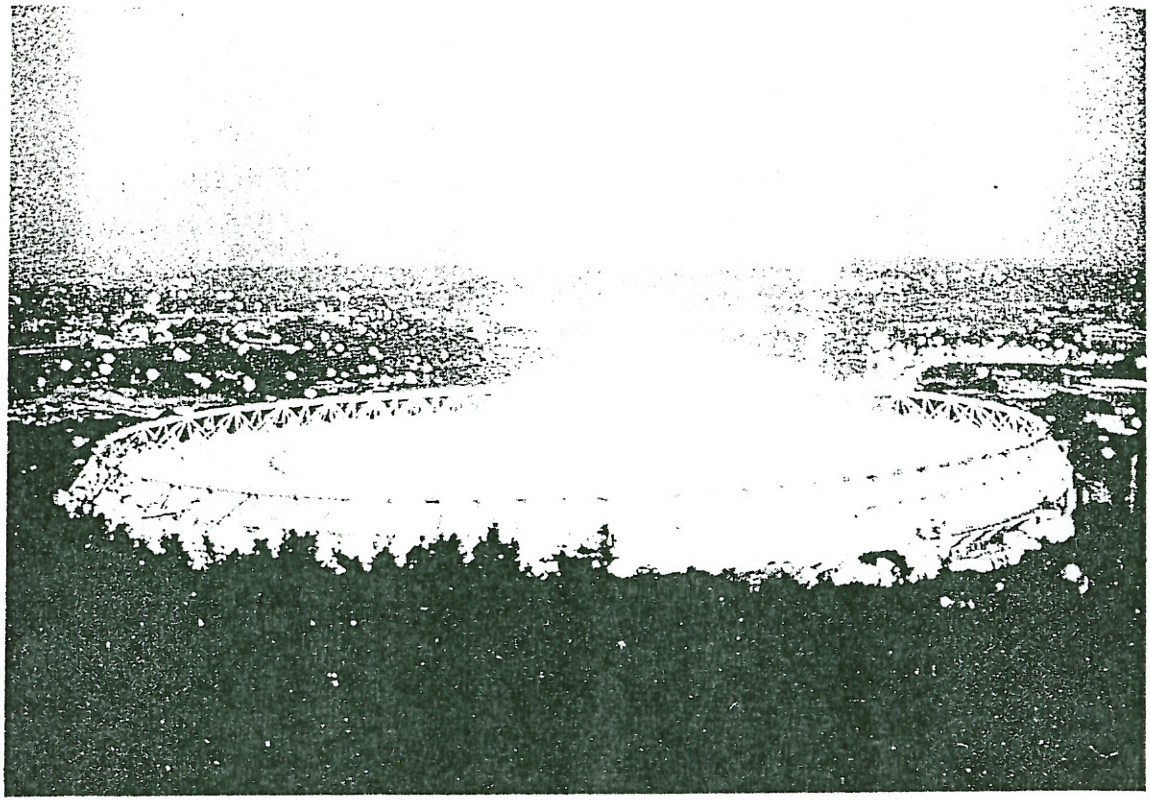

Fig. 1: A night view of the completed new roofing

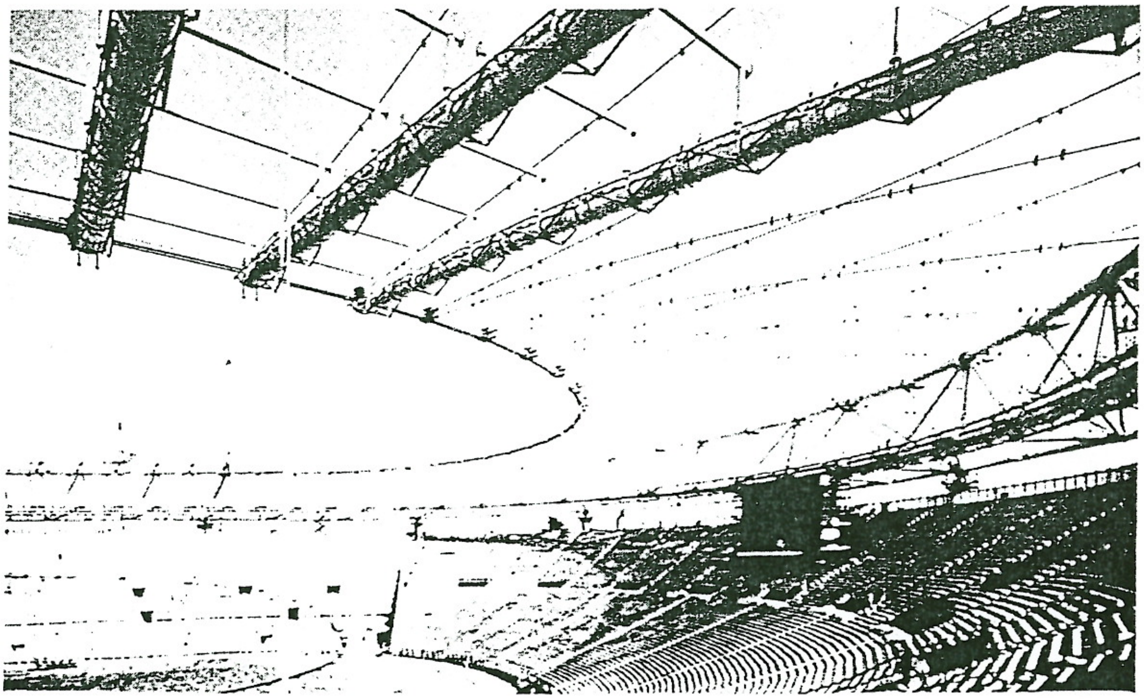

Fig. 2: Inner view of the tension ring and radial cable trusses

from the two internal elements of the compression truss and bearing the roofing panels; c) an internal tension ring, balancing the compression forces, constituted of cables (Fig. 2).

The outer trussed is constituted of high resistance steel tubes: the upper rafter (diameter 1.4 m) with a variable thickness from 60 to 70 mm is located at 36.49 m height above ground and the two lower ones (diameter 1.0 m), with variable thickness (16 to 18 mm); the cable trusses are built up by elementary wires with resistances up to 160 KN/cm^2 and diameter varying from 64 to 74 mm (for the main cables); the inner ring is made of 12 cables with 87 mm diameter, able to bear a 40,000 KN maximum operating tension.

The structural balance between those two rings allows the structural functioning with the following performances:

– very low lateral profile which is important to mitigating the visual impact;
– absence of horizontal forces in the supports due to vertical loads.

2.1 First and second order effects

The mechanical role of the tension ring consists in the transmission of an action able to maintain in tension the lower stabilizing cables under the loads weighing upon the roofing. An initial pre-stress is thus needed for the inner ring to enable the structure to bear the loads it is subjected to: as a consequence of this, the outer ring will be compressed.

The transversal-section of the roof can further provide other hints about the structural behaviour: as the cables bearing the roofing elements transmit a moment to the outer ring, like a cantilever, then consequently the ring must balance this action by means of spatial mechanism that involves the entire structural behaviour. As a matter of fact, the vertical bearings under the lower external girder are the only constraints present. The resulting action transmitted by the cable trusses to the outer ring is a distributed axial torque. Then, because of structural symmetry, the internal stress resultant will be a moment with radial axis and hence with respect to the outer ring it is mainly a flexural moment.

Neglecting now preliminarily the behaviour of the tensile structure in order to focus the attention upon the primary behaviour, one can point out that the edge beam is subjected to two kinds of actions: a more or less uniformly distributed axial torque along its perimeter, deriving from the roofing support, and a uniform compressive axial force due to the internal structure which, since it is made of cables, needs its members to be always in tension under any load condition. This implies, as outlined, the presence of a tension element (the inner ring) forcing the desired stress configuration in the structure; as a consequence of this, a dual stress configuration takes place in the external ring.

The roofing behaviour connected with the first order effects in undoubtedly the one relative to the outer ring stresses, but the behaviour of the part supporting the roofing elements must be considered from a large deflection point of view.

Cables structure show usually a significant geometrical nonlinearity; also in this case second order effects have to be considered.

A slight deflection of the inner ring causes the increase of the torque arm between the forces transmitted by the outer and inner rings. In this fact lies the concept of geometrical stiffness of the cable structures (Fig. 3).

2.2 The main stress distribution

As well known, in all tensile structures the geometrical as well as the mechanical properties depend on the initial stress: in fact equilibrium position under dead loads depends on the tensile force in the cable truss. The tensile force, on the other hand, depends on the curvature radius of the horizontal projection of the two rings. This is easily understandable keeping in mind two limit cases:

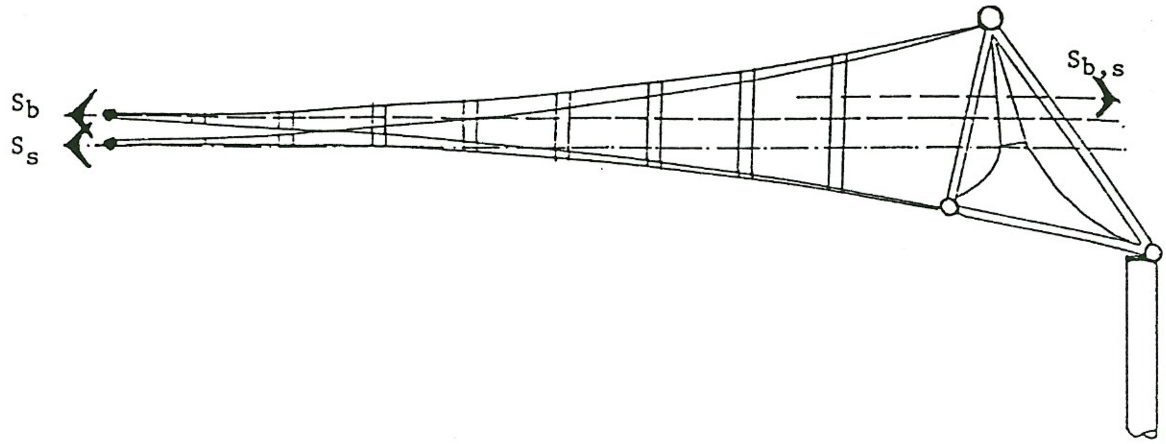

Fig. 3: A radial cross-section along a cable truss

1) the inner ring is a straight line (zero curvature), orthogonal to the cable trusses, and no transmission of normal forces arises between the two elements;
2) the inner ring has zero curvature radius (infinite curvature) and the whole force is transmitted to the radial cable truss.

It can also be noted that, the tensile force $\mathbb{S}$ in the inner ring varies proportionally to the curvature, so that its value in the bend's zone will be greater. This fact causes the torque arm needed for equilibrating all vertical loads becomes smaller, so that a greater height of the internal ring results in the bend's zone. On the whole, the spatial geometry of the tension ring will look out as a saddle-shaped.

If i_s, R_s and α_s denote respectively the distance between two successive cable trusses in the grandstand's zone, the radius of curvature in the same zone and the angle subtended by the arc i_s; i_b, R_b and α_b the same values in the bends area and $\mathbb{T}$ the tensile force in the inner ring (Fig. 4), the force $\mathbb{S}$ transmitted to the cable truss results

$$\mathbb{S} = 2 \cdot \mathbb{T} \cdot \sin\frac{\alpha}{2} \tag{1}$$

(where $\alpha = i/R$ [rad]) and since α is small the approximation $\sin\alpha/2 \simeq \alpha/2$ can be introduced so that (indicating with $\mathbb{S}_b$ the horizontal force at bends and $\mathbb{S}_s$ the horizontal force at stands)

$$\mathbb{S}_b = \alpha_b \cdot \mathbb{T} = \mathbb{T} \cdot \frac{i_b}{R_b} \tag{2a}$$

$$\mathbb{S}_s = \alpha_s \cdot \mathbb{T} = \mathbb{T} \cdot \frac{i_s}{R_s} \tag{2b}$$

and if $i_b \simeq i_s$ then

$$\frac{\mathbb{S}_b}{\mathbb{S}_s} = \frac{R_s}{R_b} \tag{3}$$

The obtained relation describes the stress distribution in the whole structure, i.e. that the ratio between the tensile forces in the cable trusses along the bends and the stands is the inverse of that of the horizontal projection of the bending radii in the corresponding zones.

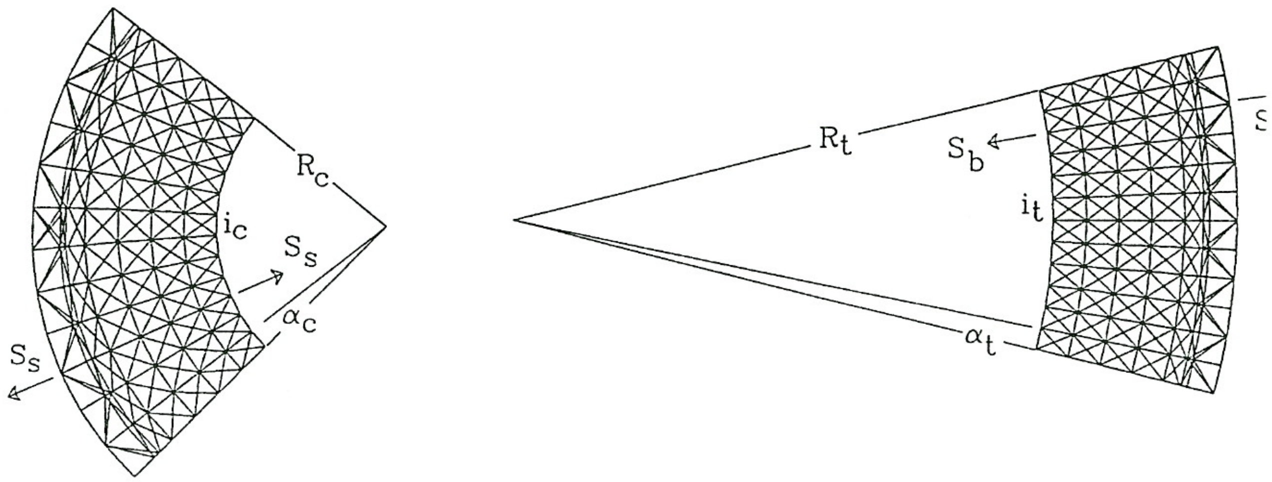

Fig. 4: Main stress distribution between outer and inner ring

By virtue of the above considerations, the structural behaviour of the roofing is generally understandable; it is eventually to be outlined the fact that the tensile force $\mathbb{T}$ in the inner ring is constant along the whole ring, as it has been implicitly assumed in the relations above written.

Besides, it can be easily shown that the outer ring is compressed by a force of the same intensity as the one of the tension ring. The stress transmission and the high resulting stiffness is obtained by means of the seventy-eight cable truss, thus working as the wheel spokes of a big bicycle.

3. WIND TUNNEL TESTS AND AERODYNAMIC BEHAVIOUR

Wind tunnel tests have been carried out at the BLWT Lab. of the University of Western Ontario on a model with 1:200 scale. The mean velocity of the flow was about 25 m/s with varying incoming direction and the following quantities have been measured by means of 170 pressure taps (44 on the underside and 126 on the topside), disposed on 8 panels of the roof (Fig. 5):

- Time histories of the local pressures for every 10° of incoming flow direction; the maximum, minimum and average values of the wind pressure have then been evaluated, as well as the root mean square of its fluctuating part;
- pressure coefficients (maxima, minima and average) for every 10° of incoming direction;
- auto and cross-spectra of the fluctuating pressure (averaged on every single panel) at the 8 instrumented panels, with flow direction varying from 0° to 360°.

The aerodynamic bahaviour shows a clear shedding phenomenon. The external border (perimeter) of the structure, constituted of the trussed compression ring with triangular cross section and tubular elements and by the roofing of the upper part of the stands, disturbs the incoming horizontal flow in such a way so that vortex shedding is built up. This causes the roofing structure to be subjected to a set of vortices with a characteristic dominant frequency. This is confirmed by the resulting Power Spectral Density Function (PSDF) of the fluctuating pressures, which shows a peak at about 0.15 Hz, almost for all the pressure taps; furthermore, the cross-correlation functions confirm the above result, showing the same peak, even if the values rapidly decrease with increasing distance.

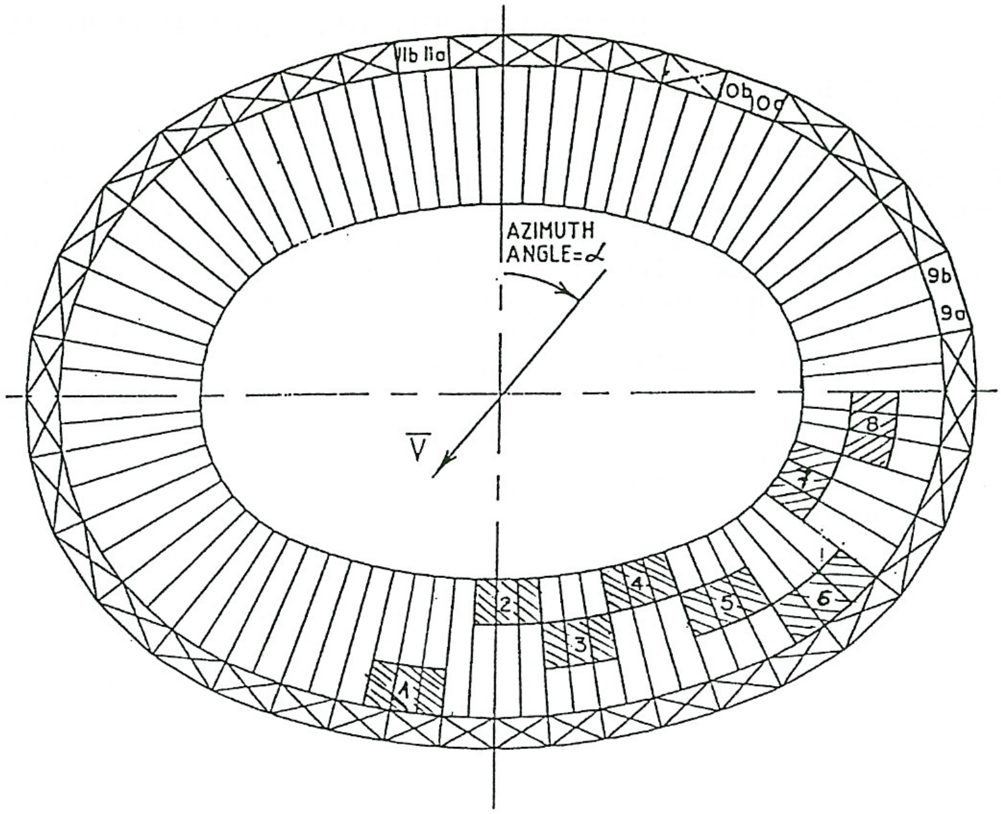

Fig. 5a: Scheme of the instrumented panels [1]

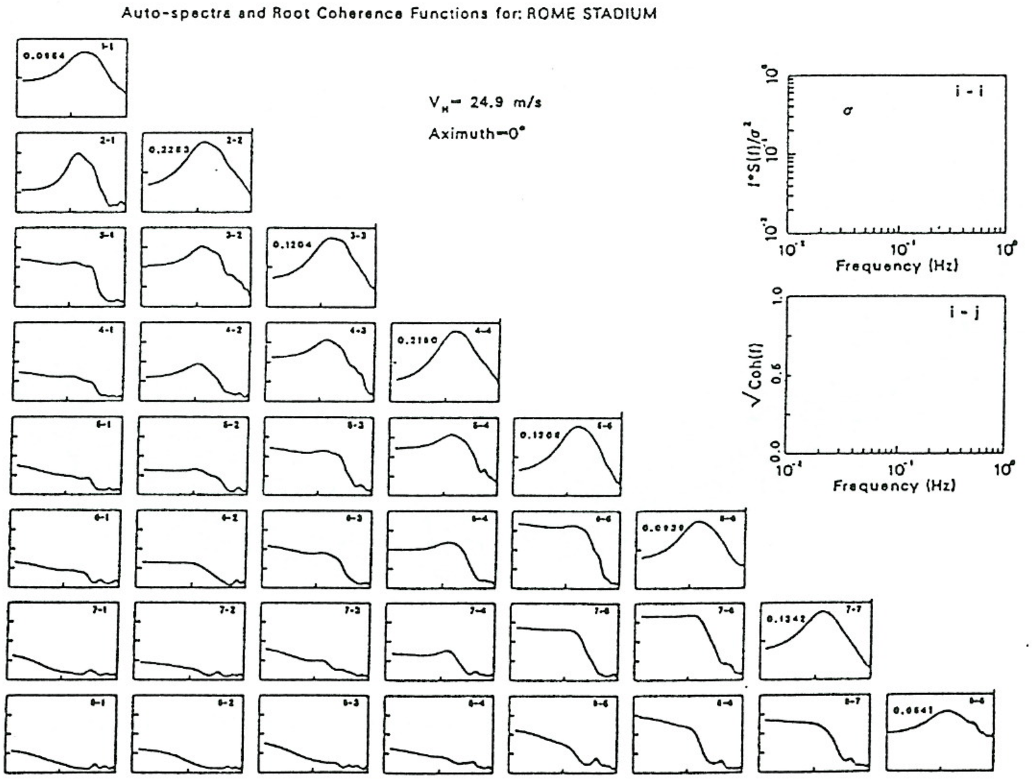

Fig. 5b: PSDF of the measured pressures [2]

4. NUMERICAL MODELING OF THE STRUCTURE

A nonlinear model of the overall structure has been developed (Fig. 6) which is composed by 796 beam elements for the outer compression ring, 2,320 cable elements for the radial cable trusses, 80 cable elements for the inner tension ring and 8 three-dimensional spring elements simulating the elastic supports at the boundary. Further 800 truss elements provide the stiffening of the roofing panels suspended on the radial cable trusses, giving a whole of 5,845 degrees of freedom (DOF) [2].

The numerical model has been developed for being analyzed by means of an extended version of FEMAS computer program [3], already employed in the recent past for wind response analyses of structures [4, 5]. In a first phase, a field of multi-correlated one-dimensional time series of the wind loading are artificially generated (s. Sect. 5). This has been done by means of the GEWIN program [6], which enables the numerical simulation of multi-correlated fields of velocities and/or pressures with given spectral properties or auto and cross-correlation. The extended FEMAS version allows a nonlinear T.D. analysis, taking into account also a first level interaction between loading and response arising from the own motion of the structure subjected to the wind.

Nonlinear static analysis for determining the equilibrium condition due to prestressing and dead weight has been performed; further the following load conditions have been analyzed, starting from the deformed (and stressed) initial configuration previously evaluated:

- uniformly distributed snow load on the whole roof;
- uniformly distributed snow load on an half structure (with reference to the major axis);
- static wind action, with reference to the average wind speed taken from the Italian Code.

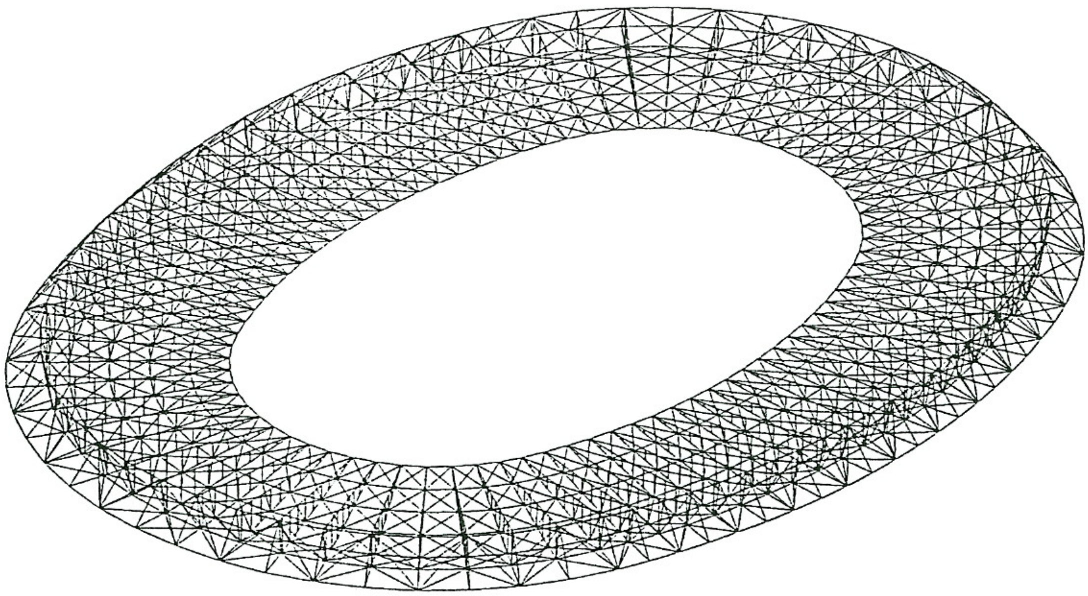

Fig. 6: Numerical model of the roofing structure

Modal analysis has brought to the values reported in Table 1, while the corresponding modal shapes are shown in Fig. 7.

Table 1
Natural frequencies of the structure

mode #	natural frequency
1	0.562 s
2	0.575 s
3	0.676 s

The nonlinear dynamic analysis was carried out by means of a direct integration procedure following the implicit Newmark method; a duration length of 100 s was chosen, with a time step of 0.1 s.

5. MODELING OF THE WIND ACTION

The generation of the wind velocity field has been done simulating 91 cross-correlated time series of the wind velocity.

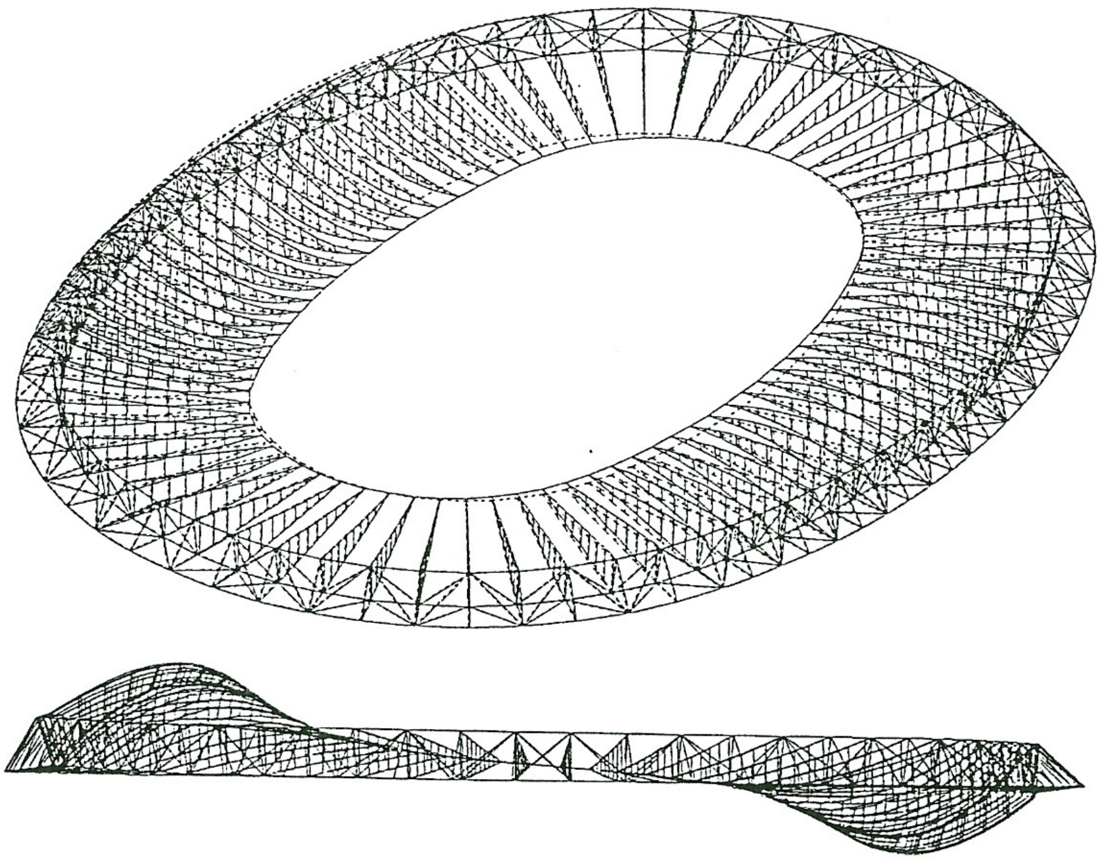

Fig. 7a: 1st modal shape ($T = 1.78$ s)

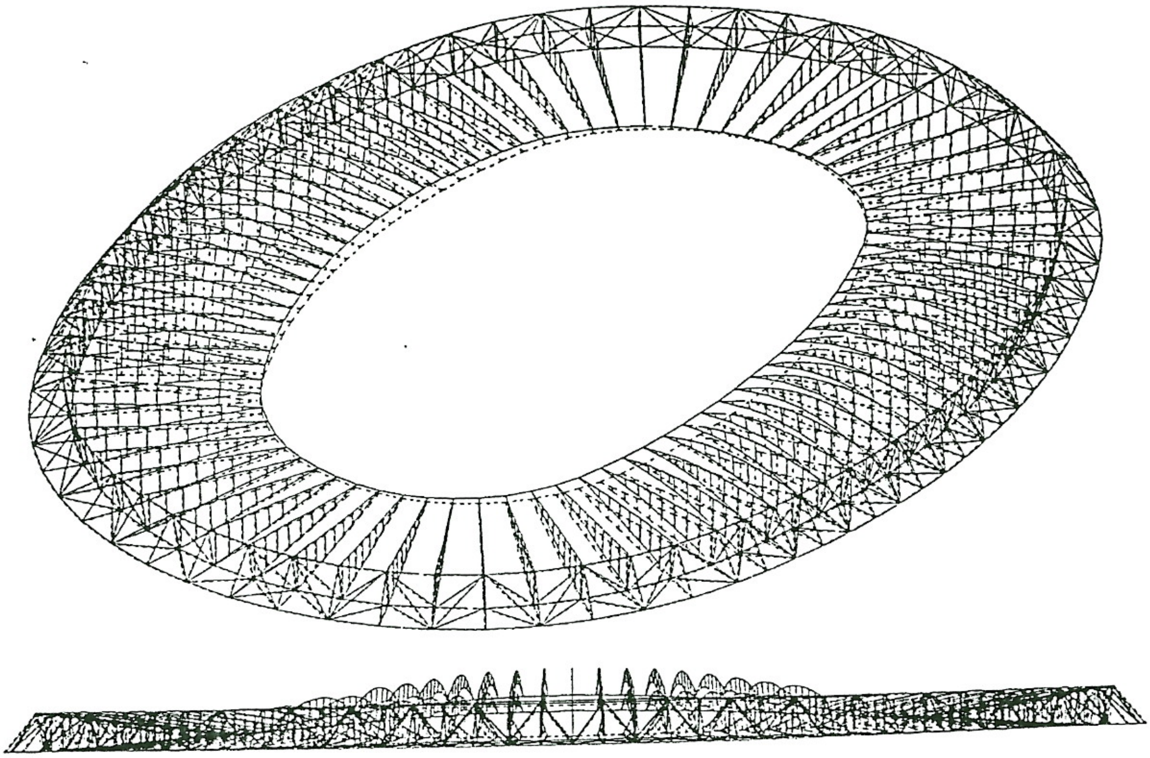

Fig. 7b: 2^{nd} modal shape ($T = 1.74$ s)

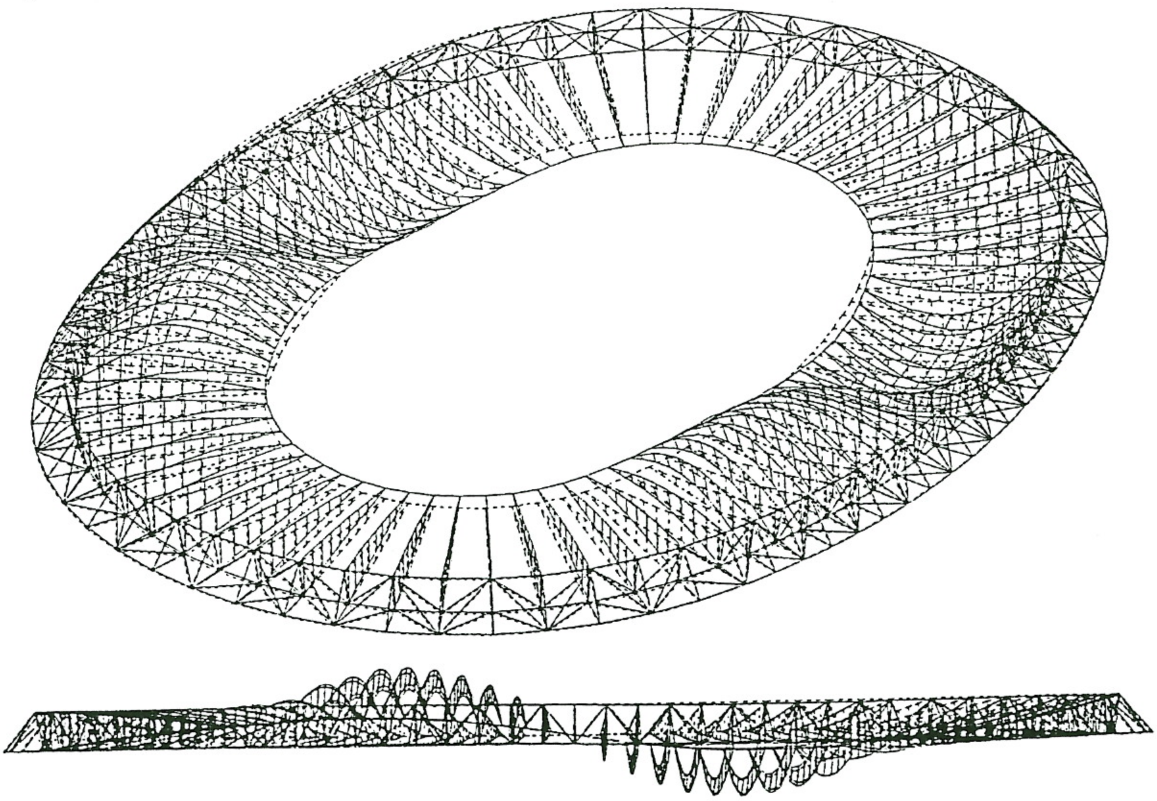

Fig. 7c: 3^{rd} modal shape ($T = 1.48$ s)

In a first phase of the study, a series of numerical simulations of the response was carried out under the following hypotheses:

- auto-spectra according to the Davenport's model;
- across-wind cross-correlation according to the root coherence function proposed by Vickery [7];
- along-wind correlation according to the Taylor's hypothesis;
- pressure coefficients as derived from the values measured by means of wind tunnel tests, taking the maximum or minimum values in order to evaluate the most cumbersome loading condition.

In a further step of the study, the measured spectra and cross-spectra of the fluctuating pressure have been considered for simulating the wind loading series, in order to reproduce as close as possible the real correlation structure of the turbulent flow.

Due to the lack of the available data, it was not possible to rebuild a complete correlation field, so that, up to now, following assumptions have been made for the PSDFs:

- auto-spectral density functions according with the measured ones;
- cross-spectral density functions according to Vickery's model and Taylor's hypothesis.

Unfortunately, due to the fact that available data did not allow to rebuild completely the structure of the cross-correlation over the whole roof, a second set of the wind loading on the structure has been generated, starting from the actual PSDF for the whole system and from the same cross-correlation as assumed in the first run.

A third numerical test has been carried out to take into account the measured correlation fields and, in particular, to consider the high values shown up to 0.15 Hz. To analyze the sensitivity of the response to this values, a modified root coherence function for the wind velocity has been used, according to those reported in Fig. 8.

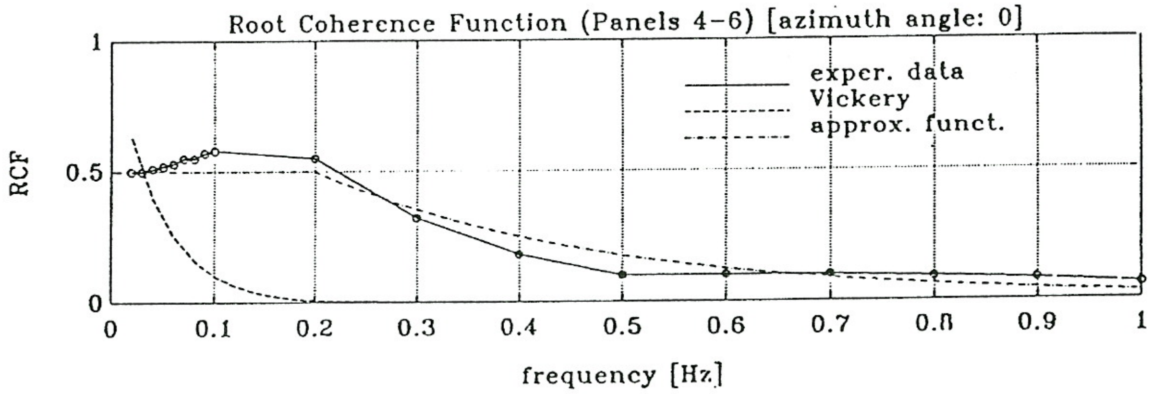

Fig. 8: Root Coherence Function: comparison between the law used in the 3rd run (approx. funct.), the Vickery's law [7] and the experimental data

6. SOME RESULTS AND COMMENTS

The obtained results show a maximum value of the displacement at the inner ring (leeward side) variable between 1.23 m (run #1), 1.32 m (run #2) and 1.37 m (run #3). In Figs. 9, 10 and 11 some results regarding the second run are shown, with reference to a point of the tension ring at leeward side, lying on symmetry axis.

From the comparison between the obtained results, the following comments can be stated:

- the effects induced by a correlation structure different from those derived from free-air coherence are limited;
- the effect of using the real PSDF instead of the theoretical one is somewhat more important. It is also to be underlined that this effect depends highly on the dominant shedding frequency with respect to the natural frequencies of the structure. So, also in the preliminary design of such a roof, the real auto-spectral characteristics should be taken into account.

It is also to be argued that experimental results carried out only on a limited part of the structure can lead to significant differences with respect to the effective characteristics of the wind. The effect of the quadrature spectra component appears to be important for this type of structures and other studies are still ongoing in order to investigate this effect on the structural response.

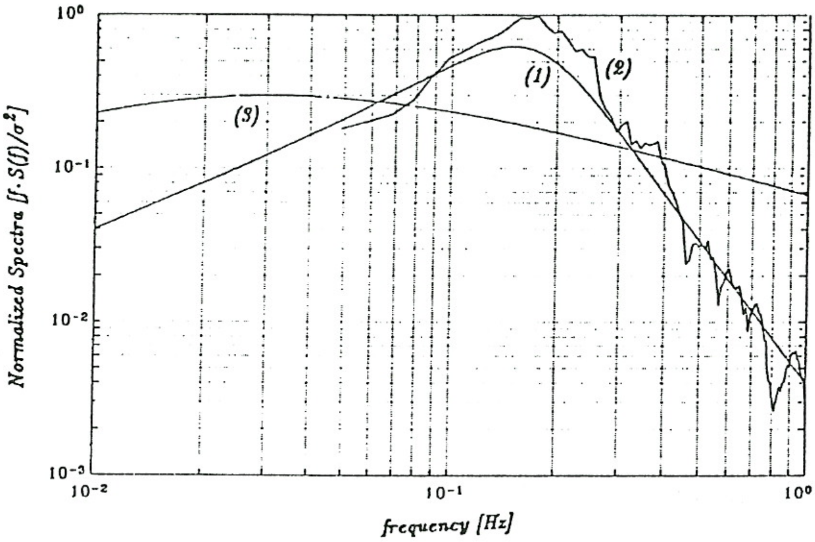

Fig. 9: Target (1), simulated (2) and Kaimal's (3) normalized spectra of wind velocity

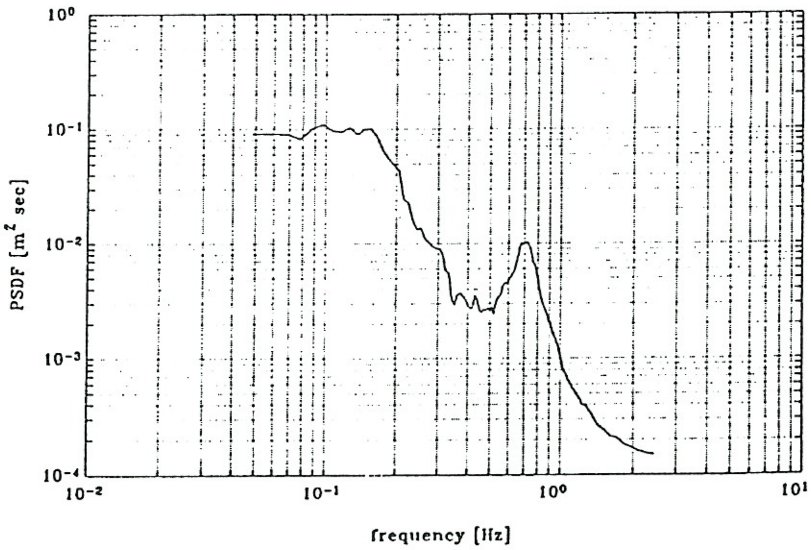

Fig. 10: Spectrum of the vertical displacement (leeward side at tension ring, run #2)

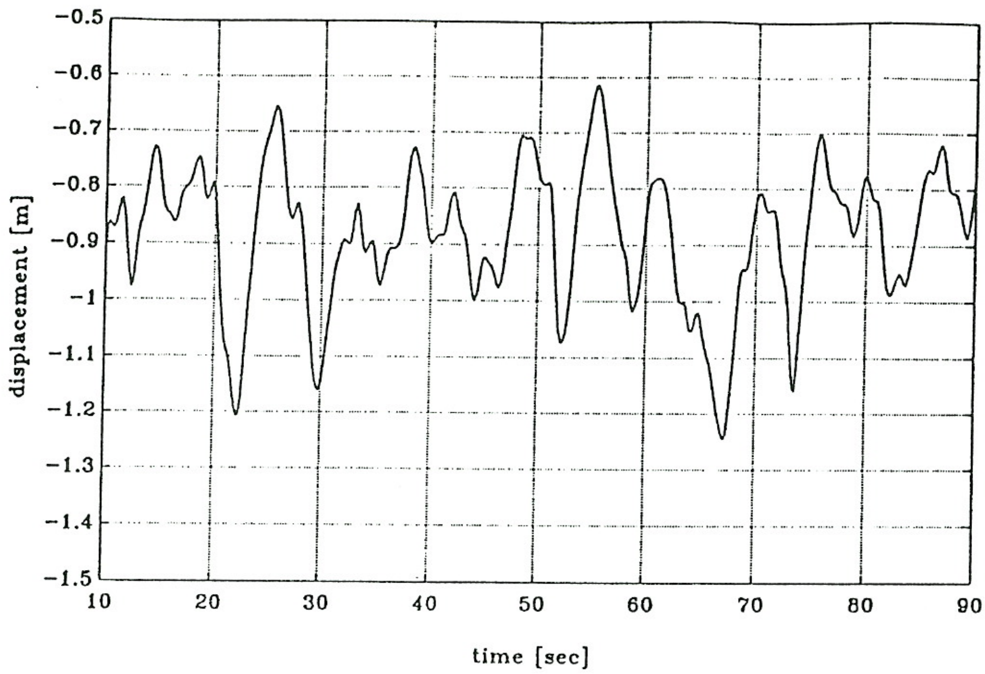

Fig. 11: Time History of the displacement (leeward side at tension ring, run #2)

7. REFERENCES

1 Vickery B.J., Steckley A., Masciantonio A., Gregoriu P.N. and Surry D., Wind tunnel study of the proposed roof for the Olympic Stadium, Rome, Italy, Final Report, BLWT-SS7-1989, Boundary Layer Wind Tunnel Lab., The Univ. of Western Ontario, London, Ontario, (1989)

2 Crocchini F., La nuova copertura dello Stadio Olimpico in Roma: il problema dell'interazione dinamica vento-struttura, Tesi di Laurea, Facoltà di Ingegneria, Università di Firenze, in Italian, (1990)

3 Beem H. et al., FEMAS - F.E. Modular Program for General Structures, Inst. für Konst. Ingenieurbau, Ruhr Univ. Bochum, (1986)

4 Borri C. and Zahlten W., Fully simulated nonlinear analysis of large structures subjected to turbulent artificial wind, Mech. of Struct. and Machines, vol. 19, No. 2 (1991), pp. 213-250

5 Augusti G., Bartoli G., Borri C., Gusella V., Spinelli P., Wind load and response of broadcsting antennas: three years of research work in cooperation with RAI, 8^{th} Int. Conf. on Wind Engrg., London, Ontario, Canada, (1991)

6 Bartoli G., Borri C., Crocchini F. and Spinelli P., GEWIN: a computer program for the generation of multi-correlated stochastic processes simulating wind time series, Dept. of Civil Engrg., University of Florence, in print

7 SimiuE. and Scanlan R.H., Wind effects on structures, John Wiley & Sons, New York, (1978)

ACKNOWLEDGEMENTS

Thanks are due to Ingg. G. Bartoli and F. Crocchini for their precious help in developing the computational model; the financial support by Ministero dell'Università e della Ricerca Scientifica e Tecnologica is also acknowledged.